RESEARCH PAPER

Development and Optimization of Plumbagin-Loaded Trastuzumab-Conjugated Silver Nanoparticles for Targeting HER2-Positive Breast Cancer Therapy

Aswathy Balan[1], Saravanan Gopal*[1]

[1*]Faculty of Pharmacy, Karpagam Academy of Higher Education, Coimbatore, Tamil Nadu, India.

***Corresponding author:** Saravanan Gopal
Faculty of Pharmacy, Karpagam Academy of Higher Education, Coimbatore, Tamil Nadu, India.
Email: Saravanan.nila@gmail.com

Abstract
Combining plumbagin with trastuzumab-conjugated silver nanoparticles enhances the stability, specificity, and therapeutic efficacy of HER2-positive breast cancer treatment. This study reports synthesising, optimising, and characterising plumbagin-loaded silver nanoparticles (AgNPs) with subsequent trastuzumab conjugation for targeted breast cancer treatment. AgNPs were synthesized via chemical reduction via the use of sodium borohydride as a reducing agent and polyvinyl pyrrolidone as a stabilizer. A Box–Behnken design within the quality-by-design framework was employed to optimize the formulation variables, identifying the polyvinyl pyrrolidone concentration as a key factor influencing the particle size and zeta potential. The optimized nanoparticles exhibited a uniform size of ~21 nm, a PDI of 0.662, and a zeta potential of −19.2 mV, ensuring stability. Plumbagin was successfully encapsulated with an efficiency of 85%, and release studies revealed a sustained, first-order release profile with ~90% drug release within 24 h, minimizing potential toxicity to healthy tissues. Surface modification with 11-mercaptoundecanoic acid introduced carboxyl groups, enabling trastuzumab conjugation through the EDC/NHS method. FTIR, SEM, TEM, and DLS analyses confirmed successful antibody attachment and structural integrity, with conjugated nanoparticles showing a size distribution of 150–170 nm. *In vitro* cytotoxic studies against MCF7 breast cancer cells demonstrated dose-dependent inhibition of proliferation, with an IC_{50} of 22.875 ± 0.733 µg/ml. AO/EB dual staining additionally confirmed the occurrence of apoptosis, confirming the therapeutic potential of trastuzumab-conjugated plumbagin silver nanoparticles as a promising targeted anticancer strategy. Plumbagin-loaded trastuzumab-conjugated silver nanoparticles demonstrated stability, sustained release, and effective anticancer activity, highlighting their potential for targeted breast cancer therapy.

Keywords: Plumbagin silver nanoparticles, Trastuzumab conjugation, Breast cancer therapy, Apoptosis induction, Targeted drug delivery

How to cite this article: Balan A, Gopal S. Development and Optimization of Plumbagin-Loaded Trastuzumab-Conjugated Silver Nanoparticles for Targeting HER2-Positive Breast Cancer Therapy. Int J Drug Deliv Technol. 2026;16(22s): 953-964. DOI: 10.25258/ijddt.16.22s.114

1. Introduction

Breast cancer remains the most prevalent malignancy affecting the female population. Its initiation and progression are influenced by complex genetic alterations involving the activation of oncogenes and the inactivation of tumor-suppressor genes, which collectively drive malignant transformation. Elucidation of the fundamental molecular signaling pathways governing tumor growth and survival provides a critical foundation for the advancement of targeted therapeutic interventions [1, 2].

Plumbagin (PLB; 2-methyl-5-hydroxy-1,4-naphthoquinone) is a bioactive compound extracted from the roots of plants in the Plumbaginaceae family. It has been shown to suppress the growth of cancer cells by triggering apoptosis, making it a potential candidate for breast cancer therapy. However, its practical use is limited by poor stability and a short shelf life. Converting plumbagin into nanoparticle form can enhance its stability, and the development of silver nanoparticles offers a promising approach for sustained drug release. These plumbagin-based silver nanoparticles may be applied in chemotherapy, although they can also affect non-target tissues [3].

Trastuzumab is a monoclonal antibody that selectively targets the HER2 receptor and is considered a fundamental agent in the standard therapy for metastatic breast cancer [4]. Its combination with chemotherapy enhances apoptotic activity, thereby improving therapeutic outcomes. When conjugated with plumbagin-loaded silver nanoparticles, trastuzumab can facilitate targeted delivery to cancer cells while minimizing exposure to healthy tissues. However, direct interaction between trastuzumab and nanoparticles is not feasible without surface modification. The presence of amine groups on trastuzumab requires complementary carboxyl groups on the nanoparticle surface to ensure effective and controlled conjugation. The introduction of such functional groups significantly improves the conjugation process and stability of the therapeutic complex [5].

2. Materials and methods

2.1. Synthesis of Silver Nanoparticles

*Author for Correspondence: Saravanan.nila@gmail.com

Silver nanoparticles were synthesized using a chemical reduction approach. A reaction mixture was first prepared by dissolving 0.1 g of $AgNO_3$ and 0.2 g of PVP in 50 ml of Milli-Q water, followed by stirring at room temperature at 1000 rpm until complete dissolution was achieved. A freshly prepared 0.05 M $NaBH_4$ solution was then made by dissolving the appropriate quantity of $NaBH_4$ in chilled Milli-Q water. This reducing agent was added slowly, drop by drop, to the PVP/$AgNO_3$ solution under constant stirring for 10 minutes. The reaction was allowed to continue for about 30 minutes to ensure full conversion of silver ions into nanoparticles. Finally, the synthesized silver nanoparticles were collected and freeze-dried for storage [6, 7].

2.2. Optimization Variables

For precise characterization of the nanoparticles, the concentrations of NaBH4, PVP, and AgNO3 were systematically varied. These parameters were chosen because of their crucial roles in the nanoparticle synthesis process. The experimental variables, where PVP (A) and silver nitrate (C) were varied between 50 and 150, and sodium borohydride (B) ranged from 20 to 60, all maintained within the defined limits. PVP functions as a stabilizing agent that minimizes nanoparticle aggregation by providing steric protection, and its concentration was adjusted from 0.1 to 0.3 g to examine its effect on particle size and stability. Sodium borohydride ($NaBH_4$) acts as a reducing agent, converting silver ions into silver nanoparticles, and its concentration was varied between 0.01 and 0.1 M to control the reduction rate as well as particle size distribution and uniformity. Silver nitrate ($AgNO_3$), serving as the precursor, was used in concentrations ranging from 0.05 to 0.2 g to evaluate its influence on nanoparticle nucleation and growth [9,10].

2.3. Optimization Study Based on a Quality by Design Approach

A Quality by Design (QbD) strategy was applied to optimize the nanoparticle formulation. The Box–Behnken design was employed to evaluate the effects of three critical factors PVP, $NaBH_4$, and $AgNO_3$ concentrations on key quality attributes, including zeta potential, particle size, and polydispersity index (PDI)[10].

2.4. Plumbagin loaded with silver

Silver nanoparticles were synthesized via a chemical reduction process by first dissolving silver nitrate and PVP in distilled water to form the reaction mixture. A freshly prepared sodium borohydride solution was then added slowly in a dropwise manner while maintaining constant stirring at approximately 1000 rpm for about 10 minutes. After formation, the nanoparticles were collected through centrifugation. Subsequently, plumbagin solution was introduced into the silver nanoparticle dispersion. [11,12].

2.5. Entrapment Efficiency

Following synthesis, the nanoparticle suspension was centrifuged, and the concentration of unbound plumbagin in the supernatant was measured using UV–visible spectrophotometry at a maximum wavelength of 420 nm [13]. The entrapment efficiency (EE%) was then determined by comparing the total amount of drug initially added with the amount of free drug detected in the supernatant, using the formula: EE% = [(total drug − free drug in supernatant) / total drug] × 100.

2.6. *In* vitro drug release study of loaded nanoparticles

The release profile of plumbagin from the nanoparticles was studied in vitro using a Franz diffusion apparatus. Phosphate-buffered saline (PBS, pH 7.4) was used as the dissolution medium to replicate physiological conditions. The nanoparticle suspension was placed in the donor compartment, which was separated from the receptor compartment by a dialysis membrane (MWCO ~12,000 Da). At fixed time intervals, aliquots were withdrawn from the receptor compartment and replaced with fresh PBS, and the quantity of drug released was measured using UV–visible spectrophotometry at 420 nm [13].

2.7. Conjugation with HER-2 Antibody (Trastuzumab)

2.7.1. Activation of Silver Nanoparticles (Introduction of a Carboxyl Group)

Silver nanoparticles were dispersed in MES buffer to obtain a concentration of 1 mg/mL. A 0.05 M solution of eleven-mercaptoundecanoic acid was then added, and the mixture was stirred at room temperature for 2 hours to facilitate the binding of carboxyl groups to the nanoparticle surface. The dispersion was then centrifuged at 10,000 rpm for approximately 10 minutes to collect the nanoparticles. The recovered particles were rinsed three times with MES buffer to remove any unbound eleven-mercaptoundecanoic acid [14].

2.7.2. EDC/NHS Activation

The carboxylated nanoparticles were redispersed in MES buffer to achieve a concentration of 1 mg/mL. Fresh EDC (0.2 M) and NHS (0.05 M) solutions were prepared in the same buffer. EDC was first introduced into the nanoparticle suspension to reach a final concentration of 0.2 M, followed immediately by the addition of NHS to obtain a concentration of 0.05 M. The reaction mixture was then incubated at room temperature for 30 minutes under gentle stirring. This step activates the surface carboxyl groups, generating NHS ester intermediates that enable subsequent conjugation with primary amine groups of trastuzumab [15].

2.8. Conjugation with trastuzumab

2.8.1. Preparation of Trastuzumab Solution

Trastuzumab was first reconstituted in phosphate-buffered saline (PBS) to obtain a final concentration of 1 mg/mL. To maintain sterility and remove any particulate impurities, the prepared solution was passed through a 0.22 µm membrane filter. This filtration step ensured that the antibody solution was free from contaminants and suitable for subsequent conjugation procedures [16].

2.8.2. Nanoparticle–Antibody Conjugation

For the conjugation process, the previously activated silver nanoparticles were combined with the prepared trastuzumab solution in a ratio of 1:10 (nanoparticles to antibody). For instance, 1 mg of nanoparticles required the addition of 10 mg of trastuzumab. The mixture was then incubated at room temperature for approximately 2 to 4 hours under gentle and continuous stirring to promote effective binding between the nanoparticles and the antibody. Alternatively, to enhance conjugation efficiency and preserve the biological activity of the antibody, the mixture could be incubated at 4°C overnight [17].

2.9. Purification of Conjugated Nanoparticles

Following conjugation, the nanoparticle suspension was subjected to centrifugation at 10,000 rpm for around 10 minutes to collect the conjugated nanoparticles as a pellet. The supernatant was carefully removed, and the pellet was redispersed in PBS. This washing process was repeated three times to eliminate any unbound trastuzumab and residual activating agents. To further improve purity, dialysis was carried out against PBS using a membrane with a molecular weight cutoff of 50 kDa. Finally, the purified nanoparticle suspension was filtered through a 0.22 µm membrane to ensure sterility [17].

2.9. Confirmation of Nanoparticle Conjugation

The successful attachment of trastuzumab to the silver nanoparticles was confirmed using multiple analytical techniques.

2.10.1. Scanning Electron Microscopy (SEM)

For SEM analysis, nanoparticle samples were prepared by depositing small volumes of the suspension onto silicon wafers, followed by drying at room temperature. A thin gold coating was applied to prevent surface charging during imaging. SEM was then used to observe the morphology of both unconjugated and conjugated nanoparticles, with particular attention given to identifying any surface modifications indicative of antibody coating [18].

2.10.2. Dynamic Light Scattering (DLS)

Dynamic light scattering was employed to measure the hydrodynamic diameter and polydispersity index (PDI) of both unconjugated and conjugated nanoparticles. An increase in particle size and PDI following conjugation served as evidence of successful antibody attachment to the nanoparticle surface [19].

2.10.3. Zeta Potential Analysis

Zeta potential measurements were conducted to evaluate changes in surface charge after conjugation. A noticeable shift in the zeta potential of the nanoparticles following antibody attachment, compared to the unconjugated form, indicated successful surface modification and the presence of trastuzumab.

2.10.4. Fourier Transform Infrared (FTIR) Spectroscopy

FTIR spectroscopy was used to analyze the chemical characteristics of unconjugated nanoparticles, free trastuzumab, and conjugated nanoparticles. The appearance of characteristic protein peaks, such as amide I (~1650 cm^{-1}) and amide II (~1550 cm^{-1}), in the spectrum of conjugated nanoparticles confirmed the presence of trastuzumab. Additionally, peaks corresponding to carboxylic acid groups from the surface modification process were also observed [20].

2.11. In Vitro Anticancer Activity of Conjugated Nanoparticles

The anticancer efficacy of the conjugated nanoparticles was evaluated using MCF-7 breast cancer cells. The cells were cultured in Dulbecco's Modified Eagle Medium (DMEM) at a density of approximately 1×10^4 cells/mL and seeded into 96-well plates. After a 24-hour incubation period to allow for cell attachment, varying concentrations of nanoparticles (5–25 µg/mL) were added. The cells were then incubated for an additional 24 hours at 37°C in a humidified atmosphere containing 95% air and 5% CO_2. Following treatment, the cells were washed, and MTT reagent (5 mg/mL in PBS) was added to each well and incubated for 4 hours to facilitate the formation of formazan crystals. These crystals were subsequently dissolved in 100 µL of dimethyl sulfoxide (DMSO), and absorbance was measured at 540 nm using a microplate reader. Cell viability percentages were calculated, and IC_{50} values were determined. All experiments were performed in triplicate to ensure accuracy and reproducibility of the results.

3. Results

3.1. Optimization of the nanoformulation

The optimization process comprised 17 experimental formulations prepared using different concentrations of PVP, sodium borohydride, and silver nitrate within defined lower and upper limits. The experimental design outlined the relative proportions of these three components for each formulation. Key parameters, including particle size, polydispersity index (PDI), and zeta potential, were determined using dynamic light scattering (DLS) and zeta potential analysis. The collected data were subsequently processed using Stat-Ease Design Expert software to identify the most suitable formulation. The outcomes obtained from the

Quality by Design (QbD) analysis are presented in Table 2.

Table 2: Optimization of variables.

		Factor-1	Fator 2	Factor 3	Response 1	Response 2	Response 3
Standard	Sample Run	A(PVP)	B (Sodium borohydride)	C (Silver nitrate)	particle size	PDI	Zeta Potential
		mg	Mg	mg	nm		mV
15	1	100	40	100	21.42	0.662	-19.2
7	2	50	40	150	61.38	0.489	-22.2
4	3	150	60	100	21.71	0.622	-21.4
9	4	100	20	50	23.24	0.634	-20.1
6	5	150	40	50	73.62	0.512	-11.57
3	6	50	60	100	74.3	0.531	-20.91
16	7	100	40	100	21.42	0.662	-19.2
8	8	150	40	150	60.82	0.501	-11.1
14	9	100	40	100	21.42	0.662	-19.2
1	10	50	20	100	98.42	0.621	-10.2
5	11	50	40	50	150	0.439	-15.62
12	12	100	60	150	57.49	0.511	-11.78
2	13	150	20	100	57.44	0.56	-15.24
11	14	100	20	150	31.64	0.529	-18.4
13	15	100	40	100	21.42	0.662	-16.49
10	16	100	60	50	20.62	0.531	-20.51
17	17	100	40	100	21.42	0.662	-19.2

ANOVA is used for the quadratic model.

The ANOVA results for particle size (Response 1) indicate that the developed model is statistically significant, as reflected by an F value of 3.70 and a p value of 0.0493, suggesting only a small probability that the observed variation is due to random error. Among the studied variables, PVP (factor A) showed a significant effect on particle size ($p = 0.0323$), highlighting its important role in controlling nanoparticle characteristics, while sodium borohydride (B) and silver nitrate (C) exhibited no significant individual influence ($p > 0.05$). Interaction terms (AB, AC, BC) were also found to be statistically insignificant, indicating minimal combined effects of these variables on particle size. Notably, the quadratic term of PVP (A^2) demonstrated a highly significant contribution ($p = 0.0036$), suggesting a nonlinear relationship between PVP concentration and particle size, whereas B^2 and C^2 were not significant. The lack-of-fit was non-significant, confirming that the model adequately fits the experimental data. Overall, the analysis emphasizes that PVP and its quadratic effect are the key factors influencing particle size, while removal of non-significant terms could further simplify the model, improve clarity, and reduce overfitting without compromising its predictive capability.

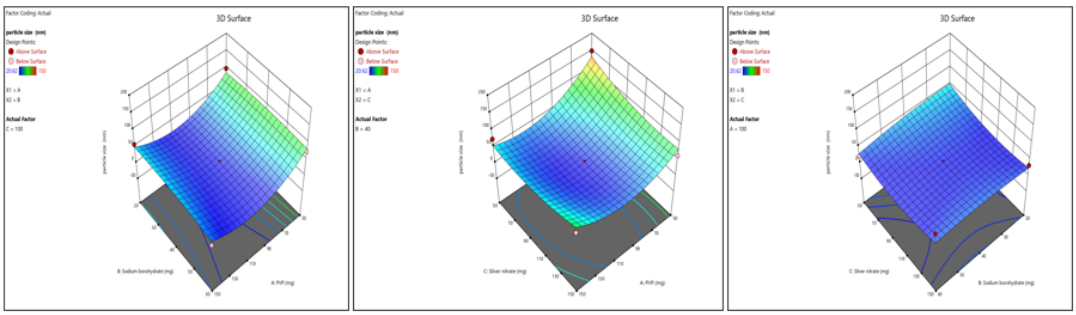

Figure 1: 3D surface response to particle size.

The ANOVA results for particle size (Response 1) indicate that the developed model is statistically significant, as reflected by an F value of 3.70 and a p value of 0.0493, suggesting only a small probability that the observed variation is due to random error. Among the studied variables, PVP (factor A) showed a significant effect on particle size ($p = 0.0323$), highlighting its important role in controlling nanoparticle characteristics, while sodium borohydride (B) and silver nitrate (C) exhibited no significant

individual influence ($p > 0.05$). Interaction terms (AB, AC, BC) were also found to be statistically insignificant, indicating minimal combined effects of these variables on particle size. Notably, the quadratic term of PVP (A^2) demonstrated a highly significant contribution ($p = 0.0036$), suggesting a nonlinear relationship between PVP concentration and particle size, whereas B^2 and C^2 were not significant. The lack-of-fit was non-significant, confirming that the model adequately fits the experimental data. Overall, the analysis emphasizes that PVP and its quadratic effect are the key factors influencing particle size, while removal of non-significant terms could further simplify the model, improve clarity, and reduce overfitting without compromising its predictive capability.

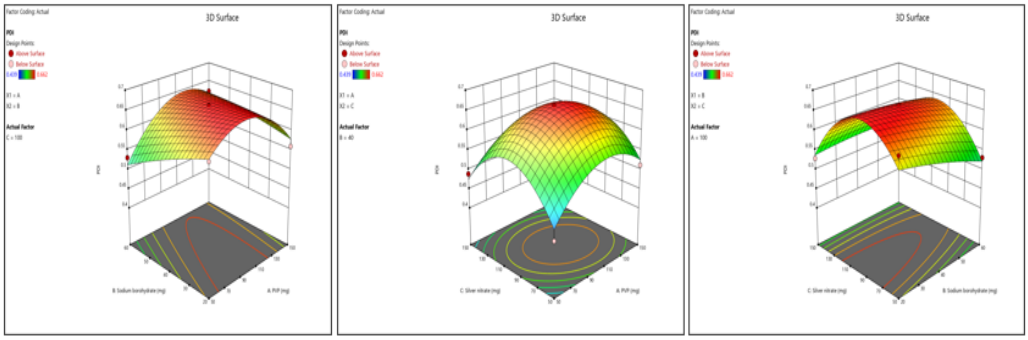

Figure 2: 3D surface response of the PDI.

The ANOVA results for zeta potential (Response 3) reveal that the model shows limited statistical reliability despite an overall p value of 0.0435. The calculated F value of 1.15 indicates that the model is not strongly significant, as there is a considerable probability that such variation could arise by chance. None of the individual factors PVP (A), sodium borohydride (B), or silver nitrate (C) demonstrated a statistically significant effect on zeta potential, as all corresponding p values were greater than 0.05. Similarly, interaction terms (AB, AC, BC) and quadratic terms (A^2, B^2, C^2) were also found to be insignificant, suggesting that neither individual nor combined factor variations had a meaningful influence on the response within the studied range. Furthermore, the lack-of-fit test was highly significant, with an extremely large F value and a very low probability of occurring by chance, indicating that the model does not adequately describe the experimental data. Overall, these findings suggest that the current model is insufficient for predicting zeta potential and may require further refinement, inclusion of additional variables, or redesign of the experimental conditions to improve its accuracy and reliability.

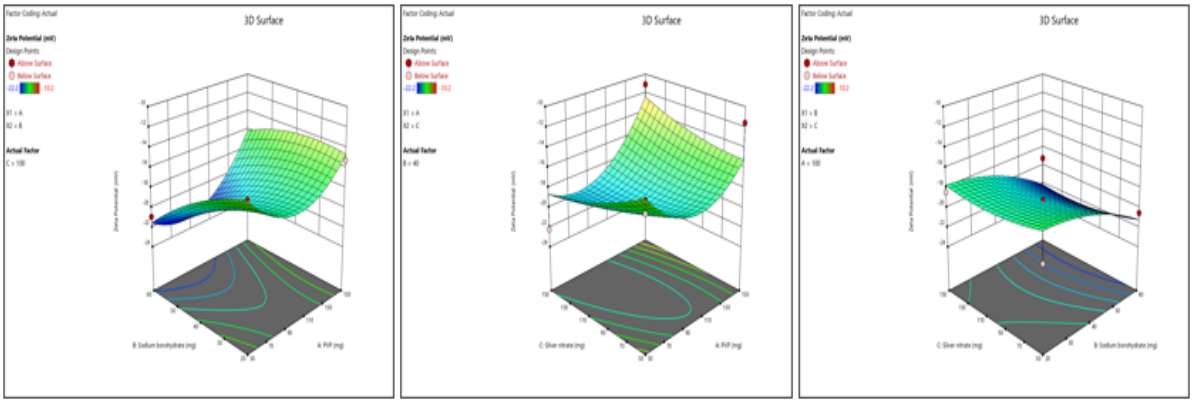

Figure 3: 3D surface response for the zeta potential.

The optimization process involved defining constraints for both formulation variables and response parameters to achieve the desired nanoparticle characteristics. The independent variables PVP (A), sodium borohydride (B), and silver nitrate (C) were each maintained within specified ranges of 50–150, 20–60, and 50–150, respectively, with equal importance assigned through weighting and significance values. Similarly, response parameters including particle size (20.62–150 nm), polydispersity index (0.439–0.662), and zeta potential (−22.2 to −10.2 mV) were set within acceptable limits to ensure optimal formulation performance. Based on these constraints, the optimization yielded a final formulation with PVP at 78.662, sodium borohydride at 39.155, and silver nitrate at 129.066. This combination resulted in a particle size of 36.284 nm, PDI of 0.606, and zeta

potential of −19.487 mV, achieving a desirability value of 1.000, indicating an ideal and well-optimized formulation.

3.2. Model Fitting Analysis for the PDI Response

In the evaluation of model fitting for particle size response, three models linear, quadratic, and cubic were compared to identify the most suitable one. The quadratic model was found to be the most appropriate, as it demonstrated a good balance between fitting accuracy and predictive performance, with an adjusted R^2 of 0.7401 and a predicted R^2 of 0.9025, reflecting strong agreement with the experimental data. Although the cubic model showed even higher R^2 values, such results indicate a risk of overfitting, which may compromise its predictive reliability. On the other hand, the linear model yielded a negative adjusted R^2 value (−0.0676), indicating a poor fit and confirming that it is not suitable for this dataset.

Therefore, the quadratic model is considered the optimal choice, as it effectively represents the data while maintaining simplicity and minimizing overfitting.

3.3. Model Fitting Analysis for the Particle Size Response

In the model fitting analysis for particle size response, three models linear, quadratic, and cubic were evaluated to determine the most suitable fit. The quadratic model emerged as the most appropriate, showing a strong balance between accuracy and predictive capability, with an adjusted R^2 value of 0.7401 and the highest predicted R^2 value of 0.9025, indicating good agreement with the observed data. Although the cubic model produced higher adjusted and predicted R^2 values, these unusually high values suggest the possibility of overfitting, which may reduce the model's reliability for prediction. In contrast, the linear model demonstrated a negative adjusted R^2 value (−0.0676), confirming its poor fit and unsuitability for describing the dataset. Overall, the quadratic model provides the best compromise by effectively capturing data variability while avoiding unnecessary complexity, making it the preferred choice for this analysis.

3.4 Model Fitting Analysis for the Zeta Potential Response

For the zeta potential response, the quadratic model was identified as the most suitable due to its strong statistical performance, with an adjusted R^2 value of 0.7540 and a predicted R^2 value of 0.9103, indicating a reliable fit to the experimental data. Although the cubic model exhibited even higher adjusted and predicted R^2 values, these elevated values suggest potential overfitting, making the model overly complex and less practical for prediction. In contrast, the linear model showed a negative adjusted R^2 value (−0.0341), confirming its poor fit and unsuitability for representing the data. Therefore, the quadratic model offers the best balance between accuracy and simplicity for describing the zeta potential response.

Entrapment Efficiency of Plumbagin

The quantity of free (unencapsulated) plumbagin present in the supernatant was determined to be 1.5 mg. Based on this, the encapsulation efficiency was calculated by subtracting the free drug from the initial 10 mg, resulting in an EE of 85%. This outcome indicates effective incorporation of the drug into the delivery system.

3.4. *In Vitro* Drug Release Study of Plumbagin-Loaded Nanoparticles

The in vitro release study demonstrated a sustained release behavior over 24 hours, with nearly 90% of plumbagin released by the end of the experiment. An initial burst release of approximately 12.5% observed within the first hour can be attributed to drug molecules loosely bound or adsorbed on the nanoparticle surface. This was followed by a gradual and controlled release phase, likely governed by diffusion from the polymeric matrix. The overall release pattern suggests effective drug retention and prolonged delivery. Furthermore, the release kinetics followed a first-order model, indicating that the rate of drug release was dependent on the remaining drug concentration within the nanoparticles.

3.5. Electron microscopy analysis (FE-SEM and HR-TEM)

Field emission scanning electron microscopy (FE-SEM) analysis, performed using a Zeiss SEM system, provided valuable information on the surface characteristics and distribution of both unconjugated and conjugated plumbagin-loaded nanoparticles. The unconjugated particles exhibited a spherical shape with a smooth surface and a fairly uniform size distribution, typically ranging between 150 and 170 nm. They were well dispersed with minimal aggregation, indicating the effective stabilizing role of PVP during synthesis. Transmission electron microscopy (TEM), carried out using a JEOL/JEM 2100 HRTEM at 200 kV, offered detailed visualization of nanoparticle morphology and structural integrity. The images confirmed that the unconjugated nanoparticles maintained a spherical shape with smooth surfaces and an approximate size of 150 nm. The absence of any surface coating in these particles suggests a lack of functionalization, serving as a reference for comparison. Additionally, the particles displayed excellent dispersion, further supporting the efficiency of PVP in preventing aggregation.

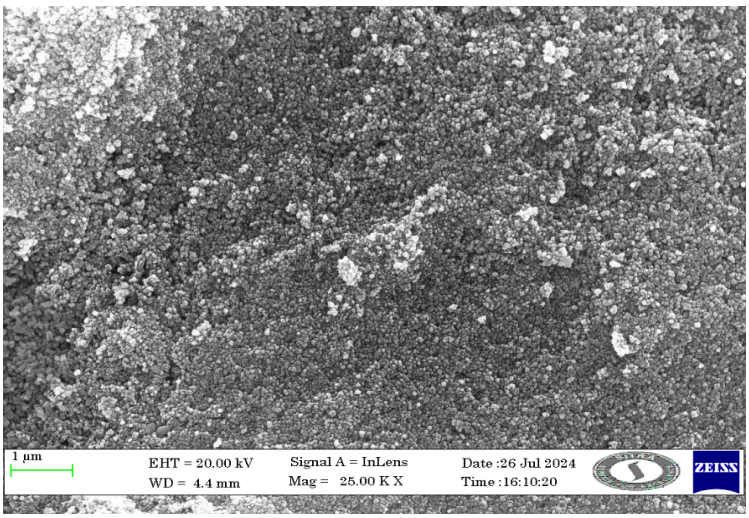

Figure 5: SEM analysis of conjugated nanoparticles.

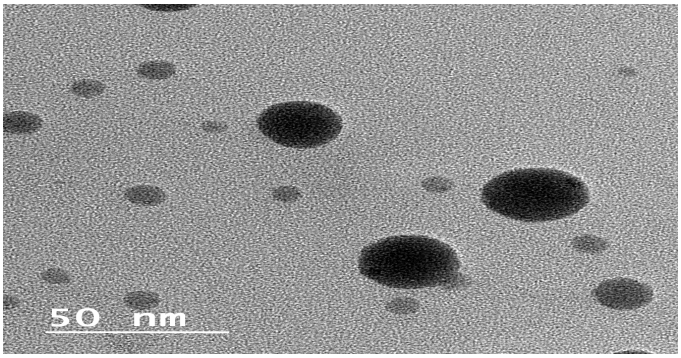

Figure 6: TEM analysis of antibody-conjugated nanoparticles in the 50 nm range.

3.6. FTIR Analysis and Interpretation of HER-2 Antibody-Conjugated Silver Nanoparticles

The FTIR spectrum of plumbagin exhibits a distinct and intense peak in the range of 1600–1700 cm^{-1}, corresponding to C=O stretching, along with characteristic signals associated with hydroxyl and aromatic functional groups. Broad O–H stretching bands are typically observed between 3200 and 3500 cm^{-1} due to hydrogen bonding, while C=C stretching of the aromatic ring appears in the region of 1450–1600 cm^{-1}. In the case of plain silver nanoparticles stabilized with polyvinylpyrrolidone (PVP), the spectrum is largely dominated by the capping agent, with a prominent C=O stretching peak around 1650 cm^{-1}. The FTIR analysis demonstrates a clear transition from unmodified nanoparticles to surface-functionalized and finally trastuzumab-conjugated nanoparticles. Successful conjugation is confirmed by the appearance of characteristic amide I and amide II bands near 1650 cm^{-1} and 1550 cm^{-1}, respectively, which are indicative of the antibody and were absent prior to conjugation. Additionally, the presence of C=O stretching related to carboxyl groups verifies effective surface modification, collectively confirming the successful attachment of trastuzumab to the silver nanoparticles.

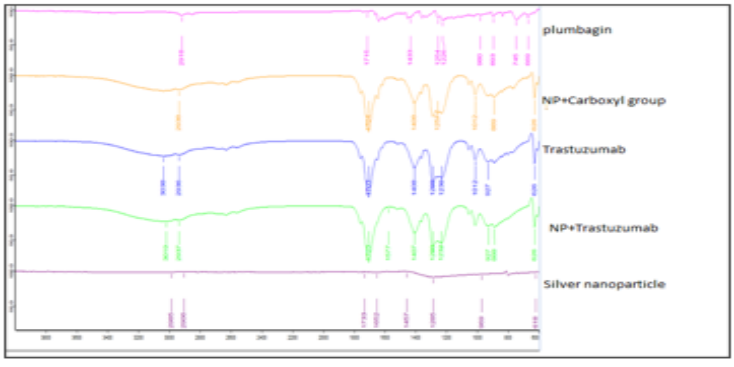

Figure 7: Characteristic peaks of plumbagin, silver nanoparticles, nanoparticles combined with carboxyl groups, and individual peaks of trastuzumab and its conjugation with nanoparticles.

3.7. *In* vitro anticancer activity of trastuzumab-conjugated nanoparticles

The cell viability results revealed a dose-dependent decrease in MCF7 breast cancer cell survival upon treatment with trastuzumab-conjugated nanoparticles. At 5 µg/ml, viability was moderately reduced compared with that of the control, while higher concentrations (10–25 µg/ml) caused a progressive and more pronounced decline in viable cells, with the highest concentration (25 µg/ml) showing the greatest inhibition of cell proliferation. This pattern indicates effective cytotoxicity of the trastuzumab-conjugated nanoparticle formulation against MCF7 cells, which correlates with increasing dosage and is consistent with previously reported trends in nanoparticle-mediated breast cancer treatments (Figures 8 and 9). These results support the potential of these nanoparticles for targeted anticancer therapy.

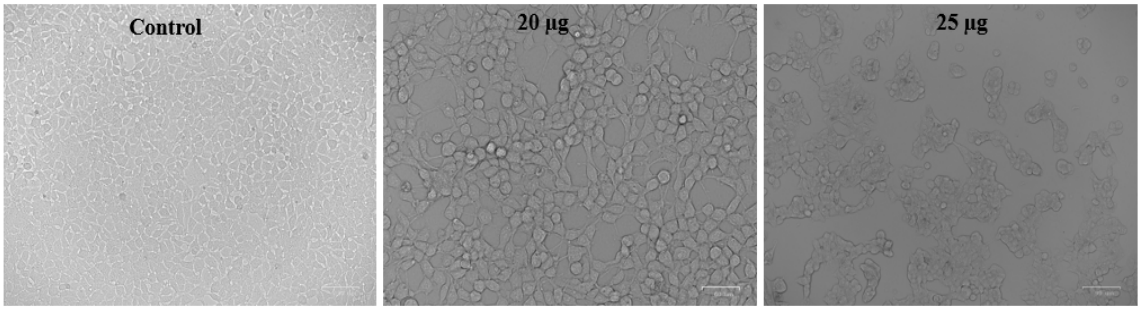

Figure 8: Morphological changes in control and trastuzumab-conjugated nanoparticle-treated breast cancer (MCF7) cells after 24 h.

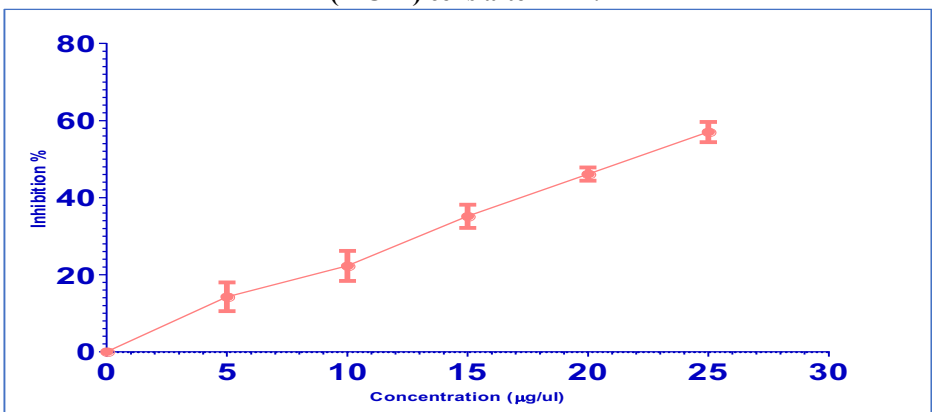

Figure 1: % breast cancer cell inhibition.

The IC_{50} value for nanoparticle treatment of MCF7 breast cancer cells was 22.875 ± 0.733 µg/ml, indicating a significant cytotoxic effect (Figure 10). The minimal standard deviation reflects consistency in the experimental results. This concentration effectively inhibited 50% of cell proliferation, demonstrating the efficacy of the trastuzumab-conjugated nanoparticles and supporting their potential as promising anticancer agents for targeted breast cancer therapy.

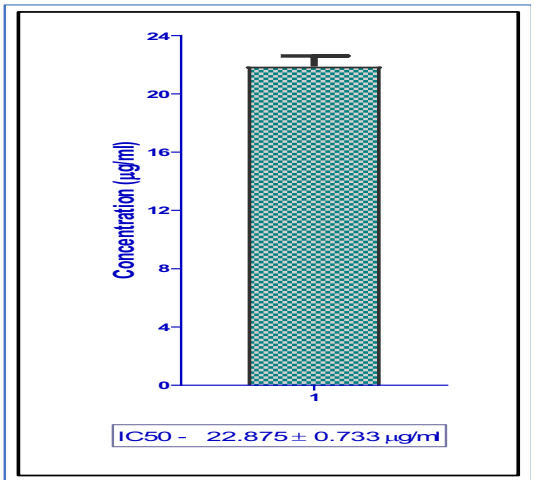

Figure 1: IC_{50} determination of nanoparticle treatment against MCF7 breast cancer cells, indicating its cytotoxic efficacy.

3.8. Evaluation of apoptosis via the acridine orange/ethidium bromide (AO/EB) dual-staining technique.

MCF-7 breast cancer cells were treated with trastuzumab-conjugated nanoparticles at concentrations of 20 and 25 µg/mL for 24 hours, after which AO/EB dual staining was performed and the cells were examined using a fluorescence microscope (Zoe Fluorescent Cell Imager, Bio-Rad) (Figure 11). Live cells exhibited green fluorescence with normal nuclear structure, while early apoptotic cells showed yellow fluorescence as a result of chromatin condensation and nuclear fragmentation. In contrast, cells in the late stage of apoptosis displayed orange to red fluorescence, indicating condensed or fragmented nuclei with uniform staining.

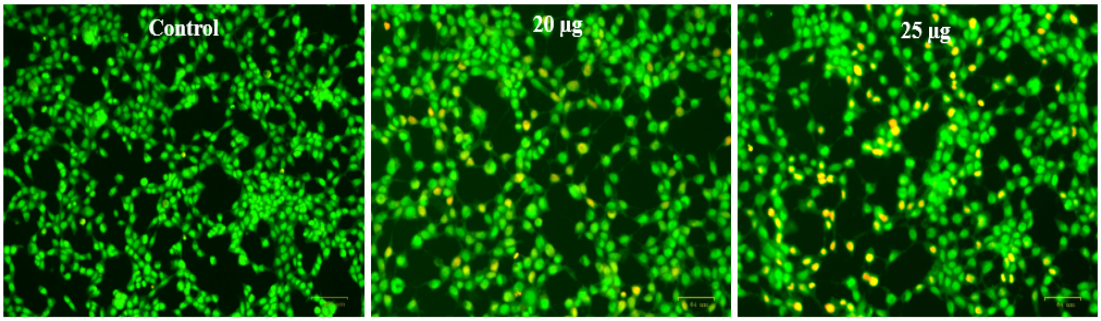

Figure 11: Assessment of the Apoptosis of MCF7 Cells via AO/EB Dual Staining.

4. DISCUSSION

The present study describes the synthesis, optimization, and characterization of plumbagin-loaded silver nanoparticles, followed by their conjugation with trastuzumab to enhance targeted therapeutic efficacy. Silver nanoparticles were synthesized through a chemical reduction method using polyvinylpyrrolidone (PVP) as a stabilizing agent and sodium borohydride ($NaBH_4$) as a reducing agent, resulting in particles with a uniform and stable size distribution. Optimization of formulation variables, including PVP, $NaBH_4$, and silver nitrate concentrations, was carried out using a Quality by Design (QbD) approach with a Box–Behnken design. The findings revealed that PVP concentration significantly influenced particle size and zeta potential, both of which are critical for nanoparticle stability and cellular uptake. The optimized formulation exhibited a particle size of approximately 21 nm, a polydispersity index (PDI) of 0.662, and a zeta potential of −19.2 mV, indicating good stability and uniform dispersion. Plumbagin was successfully incorporated into the nanoparticles with an encapsulation efficiency of 85%, demonstrating effective drug loading. In vitro release studies showed a sustained drug release profile following first-order kinetics, with nearly 90% of the drug released over 24 hours. An initial burst release of about 12.5% was observed in the first hour, followed by a gradual and controlled release from the nanoparticle matrix, which may help reduce toxicity and limit exposure to healthy tissues. A key achievement of this work was the successful conjugation of trastuzumab, a HER2-targeting monoclonal antibody, to the nanoparticle surface. This was achieved by introducing carboxyl groups using 11-mercaptoundecanoic acid (11-MUA), enabling antibody attachment through EDC/NHS-mediated coupling. FTIR analysis confirmed

successful conjugation by the appearance of characteristic amide I and II bands of trastuzumab in the conjugated nanoparticles, which were absent in unmodified samples. Morphological and size analyses using SEM, TEM, and DLS demonstrated that the conjugated nanoparticles maintained a spherical structure with a size range of 150–170 nm, while showing an increase in size and changes in zeta potential after conjugation. These observations further support successful antibody attachment. Since bare silver nanoparticles lack functional groups necessary for antibody binding, surface modification with carboxyl groups was essential to facilitate conjugation with the amine groups of trastuzumab, as confirmed by FTIR results. Overall, the study highlights the potential of trastuzumab-conjugated, plumbagin-loaded silver nanoparticles as an effective targeted drug delivery system for breast cancer therapy.

The *in vitro* evaluation of trastuzumab-conjugated nanoparticles against MCF7 breast cancer cells demonstrated a strong dose–dependent cytotoxic response, with significant reductions in cell viability at increasing concentrations. The calculated IC50 value of 22.875 ± 0.733 µg/ml reflects potent anticancer efficacy with high reproducibility of the results. Fluorescence imaging through AO/EB dual staining further confirmed the induction of apoptosis, as treated cells presented distinct morphological changes from intact green nuclei in viable cells to yellow and red/orange fluorescence in apoptotic populations. These findings suggest that trastuzumab-conjugated nanoparticles effectively inhibit MCF7 cell proliferation through apoptosis induction, highlighting their promise as a targeted therapeutic strategy for breast cancer.

5. CONCLUSION

This study demonstrated the potential of trastuzumab-conjugated, plumbagin-loaded silver nanoparticles as an effective targeted treatment strategy for HER2-positive breast cancer. The optimized formulation showed high drug encapsulation, sustained release behavior, and successful antibody conjugation, all of which contribute to improved therapeutic performance while potentially reducing adverse effects. This nanoparticle-based system offers advantages such as enhanced stability, controlled drug delivery, and selective targeting of cancer cells. The conjugated nanoparticles exhibited a dose-dependent cytotoxic effect against MCF-7 breast cancer cells, with an IC_{50} value of 22.875 ± 0.733 µg/mL, indicating strong and reproducible anticancer activity. Furthermore, AO/EB staining confirmed apoptotic cell death, as evidenced by characteristic morphological changes and reduced cell viability. These findings highlight the promise of this formulation for targeted breast cancer therapy, although further in vivo investigations are necessary to confirm its clinical applicability.

CONFLICT OF INTEREST: Nil

FUNDING: Nil

ABBREVIATION

AgNPs: Silver Nanoparticles
PVP: polyvinyl pyrrolidone
$NaBH_4$: Sodium borohydride
QbD: Quality by Design
PDI: Polydispersity Index
FTIR: Fourier transform infrared spectroscopy
11-MUA: 11-Mercaptoundecanoic acid
EDC: 1-Ethyl-3-(3-dimethylaminopropyl)carbodiimide
NHS: N-hydroxysuccinimide
SEM: Scanning electron microscopy
TEM: transmission electron microscopy
DLS: Dynamic light scattering
HER2: Human epidermal growth factor receptor 2

REFERENCE

1. Bhavsar DB, Patel V, Sawant KK. Design and characterization of dual responsive mesoporous silica nanoparticles for breast cancer targeted therapy. European Journal of Pharmaceutical Sciences. 2020 Sep 1; 152:105428.
2. Deken MM, Kijanka MM, Hernández IB, Slooter MD, de Bruijn HS, van Diest PJ, en Henegouwen PM, Lowik CW, Robinson DJ, Vahrmeijer AL, Oliveira S. Nanobody-targeted photodynamic therapy induces significant tumor regression of trastuzumab-resistant HER2-positive breast cancer, after a single treatment session. Journal of controlled release. 2020 Jul 10;323:269-81
3. Solanki R, Saini M, Mochi J, Pappachan A, Patel S. Synthesis, characterization, in-silico and *in vitro* anticancer studies of Plumbagin encapsulated albumin nanoparticles for breast cancer treatment. Journal of Drug Delivery Science and Technology. 2023 Jun 1;84:104501.
4. Rahmani F, Imani Fooladi AA, Ajoudanifar H, Soleimani NA. In silico and experimental methods for designing a potent anticancer arazyme-herceptin fusion protein in HER2-positive breast cancer. Journal of Molecular Modeling. 2023 May;29(5):160.
5. Leung JH, Tai YS, Wang SY, Fion HT, Tsung-Chin H, Chan AL. Cost-effectiveness of trastuzumab biosimilar combination therapy and drug wastage as first-line treatment for HER2-positive metastatic breast cancer. The Breast. 2022 Oct 1;65:91-7.
6. Moors E, Sharma V, Tian F, Javed B. Surface-Modified Silver Nanoparticles and Their Encapsulation in Liposomes Can Treat MCF-7 Breast Cancer Cells. Journal of Functional Biomaterials. 2023 Oct 11;14(10):509.
7. Dinparvar S, Bagirova M, Allahverdiyev AM, Abamor ES, Safarov T, Aydogdu M, Aktas D. A nanotechnology-based new approach in the treatment of breast cancer: Biosynthesized silver nanoparticles using Cuminum cyminum L. seed

extract. Journal of Photochemistry and Photobiology B: Biology. 2020 Jul 1;208:111902.
8. Beg S, Swain S, Rahman M, Hasnain MS, Imam SS. Application of design of experiments (DoE) in pharmaceutical product and process optimization. InPharmaceutical quality by design 2019 Jan 1 (pp. 43-64). Academic Press.
9. Jarullah A, Mohammed HJ. Experimental Design of Oxidative Desulfurization of Kerosene Through Response Surface Methodology (RSM). Tikrit Journal of Engineering Sciences. 2023 Jul 30;30(2):130-41.
10. Jankovic A, Chaudhary G, Goia F. Designing the design of experiments (DOE)–An investigation on the influence of different factorial designs on the characterization of complex systems. Energy and Buildings. 2021 Nov 1; 250:111298.
11. Ratan ZA, Haidere MF, Nurunnabi MD, Shahriar SM, Ahammad AS, Shim YY, Reaney MJ, Cho JY. Green chemistry synthesis of silver nanoparticles and their potential anticancer effects. Cancers. 2020 Apr 1;12(4):855.
12. Dinparvar S, Bagirova M, Allahverdiyev AM, Abamor ES, Safarov T, Aydogdu M, Aktas D. A nanotechnology-based new approach in the treatment of breast cancer: Biosynthesized silver nanoparticles using Cuminum cyminum L. seed extract. Journal of Photochemistry and Photobiology B: Biology. 2020 Jul 1;208:111902.
13. Rajkumar V, Gunasekaran C, Paul CA, Dharmaraj J. Development of encapsulated peppermint essential oil in chitosan nanoparticles: Characterization and biological efficacy against stored-grain pest control. Pesticide Biochemistry and Physiology. 2020 Nov 1;170:104679.
14. Tan G, Kantner K, Zhang Q, Soliman MG, Del Pino P, Parak WJ, Onur MA, Valdeperez D, Rejman J, Pelaz B. Conjugation of polymer-coated gold nanoparticles with antibodies: synthesis and characterization. Nanomaterials. 2015 Aug 7;5(3):1297-316.
15. Tuan TQ, Van Son N, Dung HT, Luong NH, Thuy BT, Van Anh NT, Hoa ND, Hai NH. Preparation and properties of silver nanoparticles loaded in activated carbon for biological and environmental applications. Journal of hazardous materials. 2011 Sep 15;192(3):1321-9.
16. Dinauer N, Balthasar S, Weber C, Kreuter J, Langer K, von Briesen H. Selective targeting of antibody-conjugated nanoparticles to leukemic cells and primary T-lymphocytes. Biomaterials. 2005 Oct 1;26(29):5898-906.
17. Raghav R, Srivastava S. Immobilization strategy for enhancing sensitivity of immunosensors: L-Asparagine–AuNPs as a promising alternative of EDC–NHS activated citrate–AuNPs for antibody immobilization. Biosensors and Bioelectronics. 2016 Apr 15; 78:396-403.
18. Haghighi AH, Faghih Z, Khorasani MT, Farjadian F. Antibody conjugated onto surface modified magnetic nanoparticles for separation of HER2+ breast cancer cells. Journal of Magnetism and Magnetic Materials. 2019 Nov 15; 490:165479.
19. Derakhshandeh K, Khaleseh F, Azandaryani AH, Mansouri K, Khazaei M. Active targeting carrier for breast cancer treatment: Monoclonal antibody conjugated epirubicin loaded nanoparticle. Journal of Drug Delivery Science and Technology. 2019 Oct 1;53:101136.
20. Chen LJ, Shah SS, Silangcruz J, Eller MJ, Verkhoturov SV, Revzin A, Schweikert EA. Characterization and quantification of nanoparticle–antibody conjugates on cells using C60 ToF SIMS in the event-by-event bombardment/detection mode. International Journal of Mass Spectrometry. 2011 Jun 1;303(2-3):97-102.